LAWRENCE
LIVERMORE
NATIONAL
LABORATORY

LLNL-JRNL-645374

Quasi-Continuum Photoluminescence: Unusual Broad Spectral and Temporal Characteristics Found in Defective Surfaces of Silica and Other Materials

T. A. Laurence, J. D. Bude, N. Shen, W. A. Steele, S. Ly

October 29, 2013

Journal of Applied Physics

Disclaimer

This document was prepared as an account of work sponsored by an agency of the United States government. Neither the United States government nor Lawrence Livermore National Security, LLC, nor any of their employees makes any warranty, expressed or implied, or assumes any legal liability or responsibility for the accuracy, completeness, or usefulness of any information, apparatus, product, or process disclosed, or represents that its use would not infringe privately owned rights. Reference herein to any specific commercial product, process, or service by trade name, trademark, manufacturer, or otherwise does not necessarily constitute or imply its endorsement, recommendation, or favoring by the United States government or Lawrence Livermore National Security, LLC. The views and opinions of authors expressed herein do not necessarily state or reflect those of the United States government or Lawrence Livermore National Security, LLC, and shall not be used for advertising or product endorsement purposes.

Quasi-Continuum Photoluminescence: Unusual Broad Spectral and Temporal Characteristics Found in Defective Surfaces of Silica and Other Materials

Ted A. Laurence, Jeff D. Bude, Nan Shen, William A. Steele, Sonny Ly

Physical and Life Sciences and National Ignition Facility, Lawrence Livermore National Laboratory.

We previously reported a novel photoluminescence (PL) with a distribution of fast decay times in fused silica surface flaws that is correlated with damage propensity by high fluence lasers. The source of the PL was not attributable to any known silica point defect. Due to its broad spectral and temporal features, we here give this PL the name quasi-continuum PL (QC-PL) and describe the features of QC-PL in more detail. The primary features of QC-PL include broad excitation and emission spectra, a broad distribution of photoluminescence lifetimes from 20 ps to 5 ns, continuous shifts in PL lifetime distributions with respect to emission wavelength, and a propensity to photo-bleach and photo-brighten. We found similar photoluminescence characteristics in surface flaws of other optical materials, including CaF_2, DKDP and quartz. Based on the commonality of the features in different optical materials and the proximity of QC-PL to surfaces, we suggest that these properties arise from interactions associated with high densities of defects, rather than a distribution over a large number of types of defects and is likely found in a wide variety of structures from nano-scale composites to bulk structures as well as in both broad and narrow band materials from dielectrics to semiconductors.

I. Introduction

I. a. Introduce our PL

We recently found that a photoluminescence with fast, distributed fluorescence lifetimes and broad spectral features in surface flaws on fused silica surfaces is associated with a propensity for laser damage by high fluence, ns-scale lasers[1–3]. We have found it to be associated with surfaces and nano-structured materials, particularly surfaces created by fractures[3].

The color centers (or point defects) of fused silica have been extensively studied, but the PL characteristics observed in silica surface flaws do not match either the spectral or temporal characteristics of any known point defects. Some of the spectral characteristics of this PL were observed previously[4], although information of PL lifetime was not acquired. PL from similar regions was subsequently measured in subsurface fractures upon excitation at 325 nm[5,6]. The most similar PL lifetime characteristics reported previously were from films containing Si nanoparticles[7], although it is possible

other examples may be found. The unusual properties of this PL and its association with surfaces suggest that an explanation using a distribution of isolated point defects is inadequate.

We previously proposed an explanation for the temporal properties of QC-PL that involves energy transfer interactions between neighboring defects[8]. At high defect densities, interactions between the defects can become important. We suggested that Förster Resonance Energy Transfer (FRET)[9,10] and other energy transfer mechanisms lead to the broad distribution in lifetimes observed. In particular, energy transfer between randomly distributed donors (also called sensitizers) and acceptors leads to stretched exponential decay models[11–13].

Before developing FRET-based or other models for QC-PL in more detail, in this publication we show experiments detailing the properties of QC-PL for silica, including spectral properties, lifetime distributions, and photo-induced dynamics. After describing the properties of QC-PL more completely for silica, we show examples of QC-PL in other materials. The illustrating examples from DKDP, CaF_2, and quartz suggest that QC-PL is not unique to silica. We propose that the PL we observe is associated with a high density of defects that affects both the temporal and spectral characteristics of the point defects of the host material. This high density of defects produces properties in the electronic structure that are not unique to the host material, but can be found in a variety of materials. In this interpretation, the broad spectral and temporal properties arise from the high defect density, not just from a variety of defects states. It follows from this argument that because QC-PL is linked to high spatial concentrations of defects, it can be a good metric for localized energy deposition during laser excitation and hence, correlated to damage.

II. Experimental Methods

II. a. Lifetime Imaging

Fluorescence lifetime imaging is performed as described in previous work[1]. We adapted high sensitivity confocal fluorescence lifetime microscopy for characterizing luminescence near fused silica surfaces with a wide variety of surface conditions. A pulsed laser (LDH-P-C-405B, Picoquant, Berlin) is focused using a high numerical aperture objective (UMPLFL 100X, NA=0.95, Olympus; and ED Epiplan-Apochromat, 50X, NA=0.95, Zeiss) onto a fused silica sample. Scattering and luminescence excited by the laser are collected by the same objective and focused onto a confocal pinhole (100μm). Two spectral channels (BP1: 550-610 nm; BP2: >665 nm) and a scattering channel are monitored by avalanche photodiodes (Micro Photon Devices PDM 50CT). Each detected photon is time-stamped with its absolute arrival time (100 ns resolution) and its arrival time relative to the laser pulse (150 ps for the 400 nm laser to 500 ps for the 635 nm laserincluding laser and APD response) using a time-to-digital converter (PicoHarp 300, Picoquant, Berlin). The sample is scanned in 3 dimensions using a piezo scanner (Nano-LP-200, MadCityLabs, Madison, Wisconsin), and the scanner is controlled using custom software written in LabVIEW (National Instruments, Austin, Texas) to control three analog axes (PCI-6731 And PCI-6052E, National Instruments). The experiment is synchronized with a counter-timer board (PCI-6602, National Instruments).

II. b. Simultaneous Spectroscopic and Lifetime Measurements

We determine the spectral variation of the fluorescence lifetime properties in two ways. First, we switch filters in front of the APD (480BP, 535 BP, 580BP, 620BP, and 665LP). Second, we placed a monochromator/spectrometer between the detection pinhole and the photon counting APD. The wavelength is scanned during acquisition to obtain the lifetime as a function of wavelength. Using a luminosity standard (Model 63355, Oriel-Newport, Stratford, Connecticut), the spectral profile of detection efficiency is calibrated. In this way, we obtain spectral and lifetime information simultaneously. In other measurements, we use a LN-cooled CCD camera (Princeton Instruments) to measure the spectra.

II. c. Sample preparation

The fused silica samples are prepared as described previously[14], with Vicker's indentations applied with loads between 0.5 N and 10 N. DKDP and CaF_2 samples had Vicker's indentations applied in a similar manner with the noted loads. In the experiment trying to minimize time between formation of crushed material and observation as described below, the fused silica spheres were crushed between to 50 cm fused silica samples cleaned as the other samples were.

II. d. Multi-exponential Fit for PL lifetime curve

The use of the multi-exponential model was discussed in previous publications [1,15], but is reviewed here briefly:

In order to accurately extract lifetimes, the finite bin widths, the finite measurement window available between laser pulses, and the measured instrument response must be taken into account. We take T as the time between laser pulses, and Δt as the time resolution of the histogram bins. τ_j is the lifetime of the jth component of the decay model, and IRF_i is the measured instrument response (i=0…n-1), where $\mathrm{T} = n\Delta t$. We define $r_j = \mathrm{T}/\tau_j$. A_j is the amplitude of the fitted lifetime curve (equal to the number of photons). The lifetime decay is modeled as in Zander et al. [16],

$$f_i(\tau) = \left\{ \sum_j A_j \left[e^{-i\Delta t/\tau_j} \left(\frac{1-e^{-\Delta t/\tau_j}}{1-e^{-\mathrm{T}/\tau_j}} \right) \right] \right\} * \mathrm{IRF}_i \tag{0.1}$$

The symbol $*$ denotes convolution, which is calculated using the Fast Fourier Transform (FFT). The lifetime components used for our analysis are fixed at 0.04, 0.2, 1.0, and 5.0 ns. We have found these components to be able to fit the lifetime curves we measure well with χ^2 values near 1.0.

II. e. Log-normal model for PL lifetime curve

In fitting QC-PL to multiple models, including multi-exponential models and stretched exponential models[8], we found that the distribution of lifetimes is best described in logarithmically spaced models. The log-normal model shown here has easily understood parameters that fits the data well, and can be viewed as an extension of the multi-exponential fit above to a continuous lifetime density with a normal distribution in logarithmic space:

$$P(i\Delta t,\tau_0,\sigma)=A\int_0^\infty \frac{1-e^{-\Delta t/\tau}}{1-e^{-T/\tau}}\exp\left[-i\Delta t/\tau-\left(\ln \tau/\tau_0\right)^2\Big/2\sigma^2\right]\frac{d\tau}{\sqrt{2\pi}\tau\sigma} \tag{0.2}$$

We convert this expression to logarithmically spaced lifetimes $u=\log_{10}\tau$ to obtain:

$$P(i\Delta t,\tau_0,\sigma)=A\int_0^\infty \frac{1-e^{-\Delta t 10^{-u}}}{1-e^{-T10^{-u}}}\exp\left(-i\Delta t 10^{-u}\right)\exp\left[-\left(u-\ln\tau_0/\ln 10\right)^2\Big/2\left(\sigma/\ln 10\right)^2\right]\frac{du}{\sqrt{2\pi}\,\sigma/\ln 10} \tag{0.3}$$

The photon density as a function of u for this distribution is simply Gaussian:

$$h(u)\,du=\exp\left[-\left(u-\ln\tau_0/\ln 10\right)^2\Big/2\left(\sigma/\ln 10\right)^2\right]\frac{du}{\sqrt{2\pi}\,\sigma/\ln 10} \tag{0.4}$$

III. Results

We first present experiments and analysis that demonstrate the defining properties of QC-PL for the case of fused silica surface flaws. The five defining properties of QC-PL are as follows. First, QC-PL is found at surfaces of materials – it is most prevalent in regions with significant surface flaws, containing fractured or crushed material. Second, QC-PL has broad excitation and emission spectra, with no clearly identifiable spectral lines. Third, there is a broad distribution in photoluminescence lifetimes that typically span from about 20 ps or lower to about 5 ns. Fourth, there is often observed a continuous shift in PL lifetime with respect to emission wavelength – emission peaks are slightly red-shifted with respect to the excitation wavelength. Fifth, there is a marked propensity for QC-PL to photo-bleach (although not completely) and to photo-brighten during exposure to laser excitation. After providing details on these properties for silica, we also present a series of experiments that show that these characteristics are observable in other optical materials.

III. a. Spectral properties

Regions of fused silica surfaces with QC-PL exhibit relatively broad emission spectra that do not have readily identifiable spectral lines. Figure 1 shows emission spectra acquired for a 10N Vicker's indentation on a fused silica surface excited at four wavelengths. In this example, excitation with 3.1 eV (black line) leads to a broad emission peaking at about 2.4 eV with a FWHM width of around 0.7 eV. As the excitation energy decreases (2.7 eV, red line; 2.3 eV, green line; 1.95 eV, cyan line; blue line discussed later), the emission peak energy likewise decreases (inset shows peak position). No consistent, readily identifiable peaks are observed.

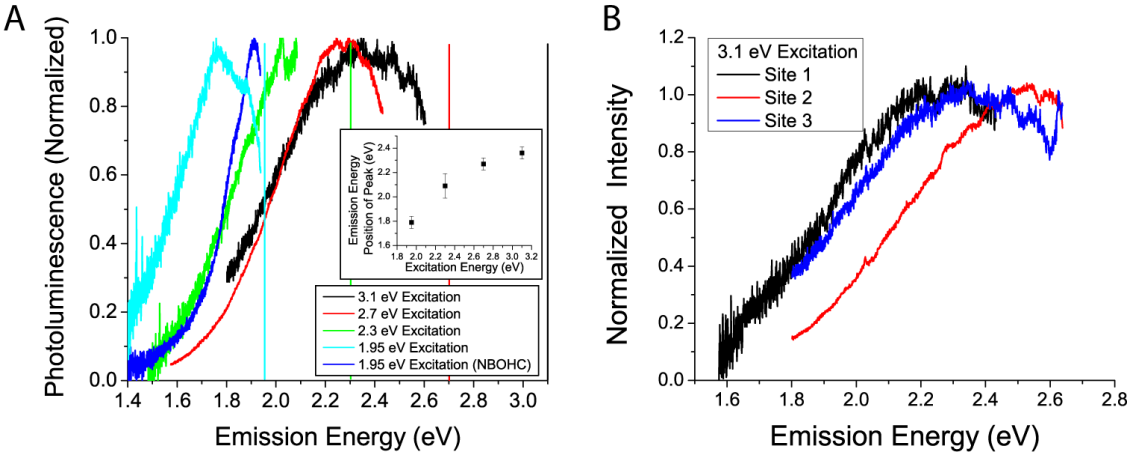

Figure 1: A. Spectra of Vicker's indentations on fused silica surface as a function of excitation energy, calibrated by use a blackbody light source. Excitation lasers used include 400 nm (3.1 eV), 470 nm (2.7 eV), 543 nm (2.3 eV), and 633 nm (1.95 eV). The blue line is a spectrum from a region of a laser-induced damage site on silica that exhibits the Non-bridging Oxygen Hole Center (NBOHC) [4]. B. Three different Vicker's indentations on silica surfaces exhibit different spectra that do not allow spectroscopic assignment of lines.

Spectra with the same excitation wavelengths do not necessarily have consistent emission maxima or spectral features (Figure 1B). For example, the spectra acquired for regions in three different 10N Vicker's indentations on silica surfaces do not have peaks at the same energy, preventing the assignment of the observed PL with a new, previously unknown defect.

We use the non-bridging oxygen hole center (NBOHC) defect as a counter-example, illustrating how a known silica point defect is observed under these conditions (blue line, Figure 1A). The NBOHC defect [17,18]is also observed in certain regions of a laser-induced damage site in fused silica (Figure2) [Ref=?]. Figure 2A shows the 2D map of PL intensity for a 3D confocal scan (integrating over the z axis), with 1.95 eV pulsed excitation (635 nm). Figure 2B is the map of PL intensity for PL lifetimes in the 40 ps to 5 ns range, and the characteristics are those of QC-PL. For PL with much longer lifetimes (Figure 2C), the PL intensity is localized in a smaller, doughnut-shaped region. The PL in this region has the spectral characteristics of the NBOHC defect (shown in Fig. 1A), and the fluorescence lifetime of this defect matches the known value of the NBOHC of 13 μs (not shown). QC-PL has a broad spectrum of lifetimes with no clear structure and does not allow simple identification as in the case of the NBOHC.

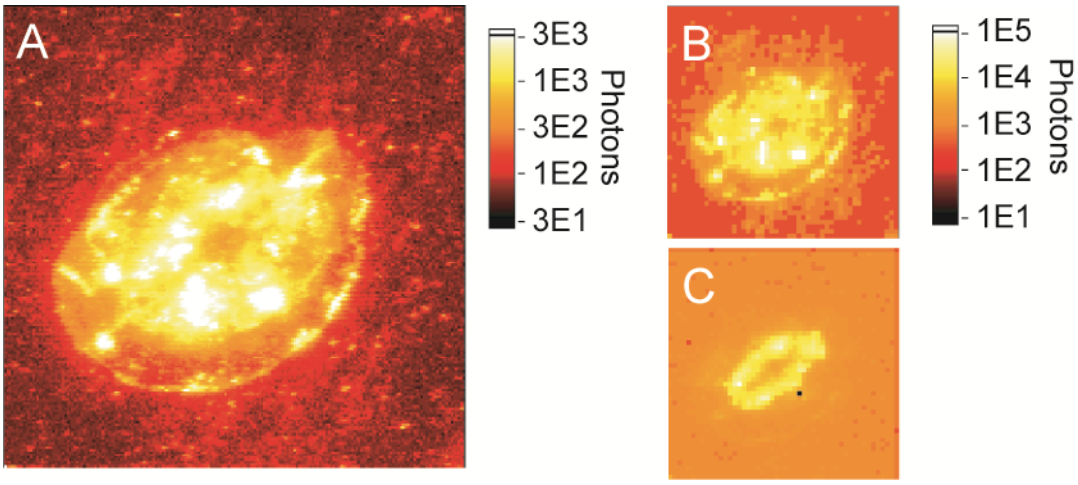

Figure 2: A. Image of laser-induced damage site in fused silica excited by 635 nm laser (1.9 eV). This laser excites the NBOHC silica defect efficiently. **B**. Image of PL exhibiting QC-PL lifetime components (0.4-5 ns). C. Image of components with slow lifetimes (>> 25 ns, not resolved in this experiment). Slow lifetime components have a different spatial distribution than the QC-PL components. Further measurements reveal the spectrum (Fig. 1A) and lifetime (13 µs, not shown) of the NBOHC for the PL from the central region of the damage site shown in C.

III. b. Lifetime data indicate a broad distribution of temporal decay rates

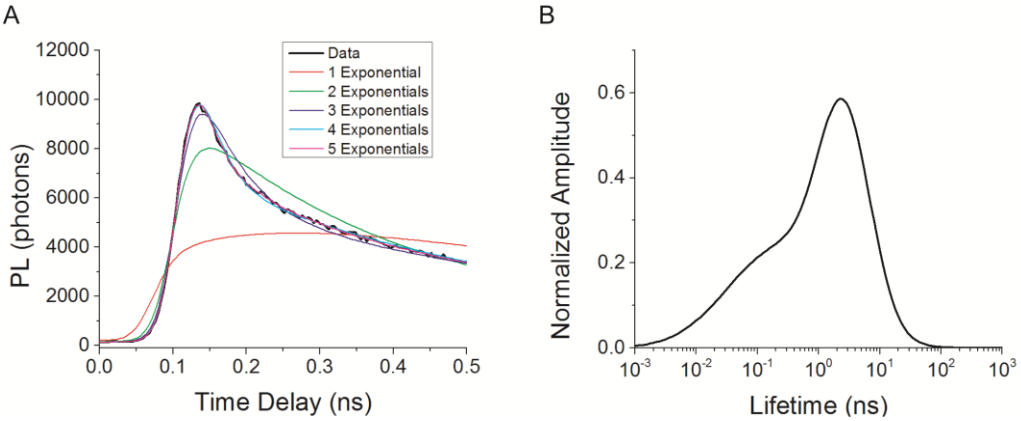

Figure 3: A. Fluorescence lifetime decay of 2N silica Vicker's indentation is fitted a series of multiple exponential functions, accounting for instrument response and finite bin widths. The measurement was performed using a doubled Titanium-Sapphire laser to minimize the instrument response. B. Distribution of lifetimes fitted using a log-normal function. Two log-normal components were required to fit the data.

As shown in our previous work [1], QC-PL exhibits a broad distribution in PL lifetimes. In this section, we show measurements performed using a doubled Titanium Sapphire laser tuned to 800 nm to minimize the instrument response; in this case, the instrument response is dominated by the APD detector (~50 ps) rather than the laser pulse as in our other measurements. Figure 3 shows the fluorescence lifetime curve measured from a 2N Vicker's indentation on fused silica. A series of fits with an increasing number of components is shown in Figure 3A. The fits resulted in χ^2 values of 75, 8.1, 2.2, 1.60, and 1.55 for the

one-, two-, three-, four-, and five-component fits, respectively. Four components were required to fit the data well, with only marginal improvement of the fit when adding the fifth component. For the quality fits, the lifetimes fitted ranged from 20 ps to 5 ns for the four-component fit, and from 10 ps to 5 ns for the five-component fit. These fits support the previous finding that there is a broad distribution in lifetimes.

We performed additional fits using a model with a distribution in lifetimes. We use a log-normal distribution in lifetimes to model the lifetime curves. Previously, we also used a stretched exponential model to fit lifetime data for QC-PL[8]. However, we have found the interpretation of parameters simpler for the log-normal distribution without compromising fit quality. For this lifetime curve, two log-normal components were required to obtain an adequate fit ($\chi^2 = 1.7$). The distribution in lifetimes (from ~10 ps to ~10 ns) matches the multi-exponential fit well. These results illustrate the large, continuous distribution in fluorescence lifetimes found in QC-PL, indicating an extremely heterogeneous environment for the defects.

III. c. Continuous shift in PL lifetime as function of spectrum

We measure the variation of the PL lifetime curves as a function of spectrum in order to understand if the distribution in lifetimes observed indicates a common origin for the entire PL spectrum. We often find very little change in the lifetime distribution as a function of emission energy. However, there are also cases where there is a continuous shift in the lifetime as a function of emission energy. These cases are typically observed in situations where photo-brightening has occurred (see next section).

In this section, we measure PL lifetime as a function of spectrum by manually switching between various bandpass and longpass filters (Figure 4). Figure 4B, which shows the lifetime distributions fitted for the lifetime curves in Figure 4A, shows that higher emission energies have faster initial decays than lower energies. This consistent pattern is observed often enough in QC-PL that we define it as a key characteristic. As explained in a future publication, this characteristic may be explained by interactions between defects[8], where delays in the emission from longer emission are caused by successive energy transfer events as the excitation trickles down to defects with lower energy.

For the same spectral range of emission, PL lifetimes are clearly affected by the excitation energy. For the 665 nm longpass (Figure 4C), the 400 nm excitation had shorter lifetimes than the same spectral range with 635 nm excitation. This suggests that different populations of defects are excited by the different excitation lasers.

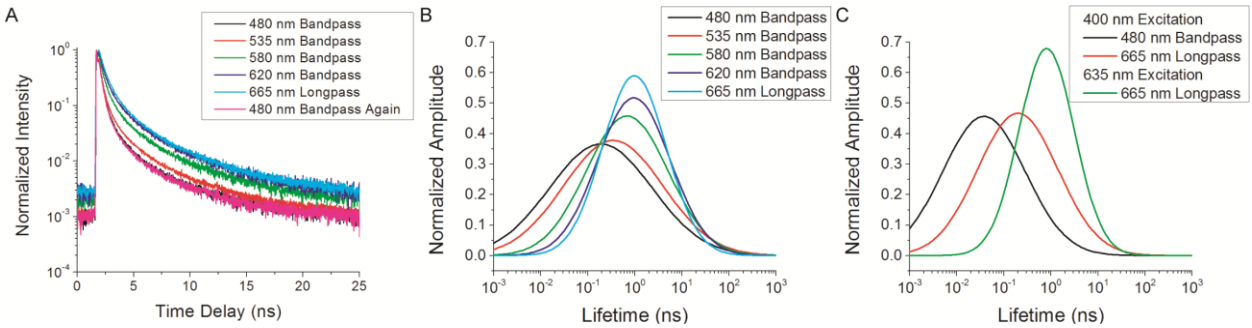

Figure 4: Fluorescence lifetime curves often vary as a function of emission wavelength (energy). **A**. PL lifetime decay for 2N Vicker's indentation on fused silica surface as a function of emission wavelength (using bandpass filters). **B**. The distribution of lifetimes narrows and shifts to longer lifetimes for longer wavelengths (lower energies). **C**. The distribution in lifetimes is also different for same emission spectral range when excited by different excitation energies.

III. d. Propensity to photo-bleach and photo-brighten

We observe a photo-reactivity in QC-PL which illustrates the importance of the local surface properties of the material to QC-PL. During a long-time exposure of a single site to the full probe laser intensity (150 kW/cm^2), we most often observe photo-bleaching of the QC-PL as shown in Fig. 5A. There are often small "bursts" of luminescence observed, momentary spikes in the intensity (Fig. 5A). More interestingly, at certain positions usually along fractures, a dramatic photo-brightening can be observed. For example, after observing the photo-bleaching and subsequently obtaining the image in Fig. 5A, the laser focus was moved by stepper motor to a fracture (at red line in Fig. 5B), and within seconds the intensity increased by a factor of 50. After photo-brightening, the photo-brightened spot is visible in a subsequent image (inset, Fig. 5B), excluding experimental artifacts as the cause of observing photo-brightening. As can be seen in Fig. 5C, as photo-brightening occurs, the luminescence lifetime decreases. The photon detection rates are low enough that pileup in time-correlated single photon counting cannot explain this lifetime change. The shifts in fluorescence lifetime to shorter lifetimes occur for the entire emission spectrum. Even though the lifetimes in different parts of the spectrum may shift continuously as described in the previous section, the entire spectrum shifts together.

As shown in Fig. 5D, the photo-brightening effect depends on the laser excitation intensity. Decreasing the laser excitation intensity by a factor 3 stops the photo-brightening process (green arrow near 5 s), but the photo-brightening process continues as before when the laser excitation intensity is returned to the original value (red arrow near 20 s).

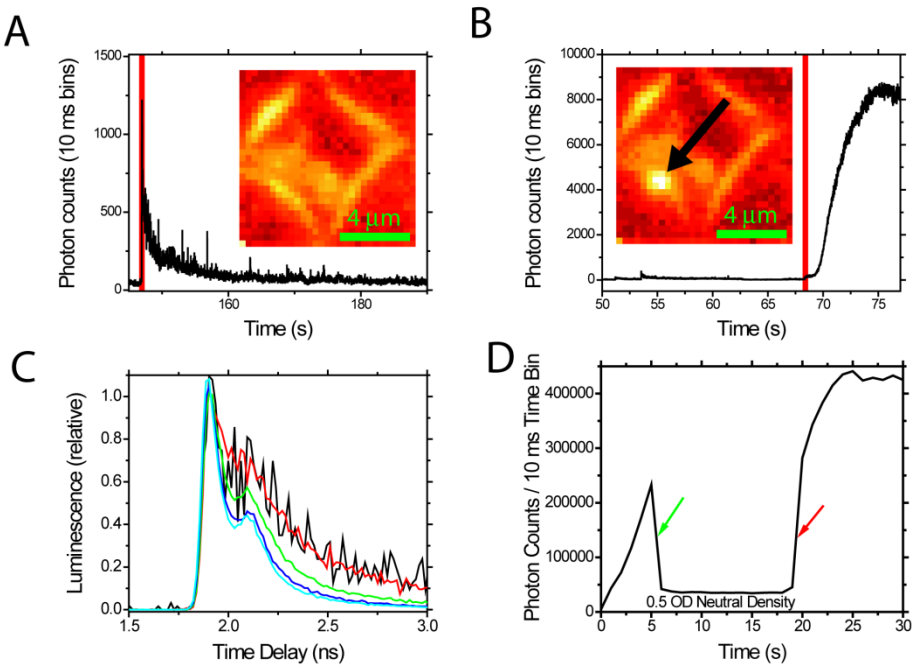

Figure 5: QC-PL exhibits photo-bleaching and photo-brightening. In A and B, the vertical red line indicates the movement of the stepper motor stage to the final position of the time trace. **A**. Time trace of luminescence from 0.5 N indent on fused silica. Photo-bleaching is most often observed. Inset image was acquired after photo-bleaching. **B**. Time trace of luminescence from same indent as in A, but at the fracture site indicated in inset image taken after photo-brightening. Rapid photo-brightening is observed after movement of the stage. **C**. Normalized fluorescence lifetime curves for five 1-second intervals after movement of the stage (red line). Black: 0-1 s. Red: 1-2 s. Green: 2-3 s. Blue: 3-4 s. Cyan: 4-5 s. Lifetime distribution shifted to shorter times. **D**. The rate of photo-brightening is dependent of laser excitation intensity. Increase in signal is stopped by reduced excitation intensity by adding a 0.5 OD neutral density filter (green arrow). Removal of the ND filter causes increase in signal to resume (red arrow). Signal saturates soon afterward.

III. e. These properties found in fractured silica appear in other optical materials as well

QC-PL is found in other optical materials, indicating that it is not a feature specific to fused silica, but is a general feature of surfaces under certain conditions. Fractures and crushed materials are particularly prone to exhibiting QC-PL, as illustrated in Fig. 6. Figure 6 shows measurements performed on other optical materials. Figures 6A,B, and C show images of Vicker's indentations on CaF_2, DKDP and Quartz, respectively. Bright PL is observed in the fractured regions. In Fig. 6D, a Vicker's indentation on CaF_2 does not exhibit increased PL since there was no fracture (0.5 N force was used rather than 10 N in Fig. 6A). This shows the importance of fractures for producing QC-PL[3], and also shows that the PL observed is not due to contamination of the Vicker's indentation tip.

Photo-bleaching and photo-brightening are also observed in these materials. Photo-brightening occurred in DKDP (Fig. 6E) and quartz (Fig. 6F), but we only observed photo-bleaching in CaF_2. The "bursts" of luminescence seen in fused silica are also seen in DKDP. A subsequent image shows the brightened spot (Fig. 6E inset). For calcium fluoride, we were able to observe photo-bleaching and "bursts", but not photo-brightening. Photo-brightening to a smaller extent (a factor of 2) was reported previously for fluorescent quantum dots[19].

Simultaneous spectral and lifetime information are obtained by using a monochromator/spectrometer to scan through wavelengths over a large range. The monochromator method reduces signal, but allows for accurate spectral resolution and obtains simultaneous lifetime and spectral data. The distributions in PL lifetimes spanned similar ranges to those found for fused silica (Fig. 6G). DKDP exhibited a PL lifetime distribution with longer lifetimes, but upon photo-brightening the lifetime distribution was much shorter (green dotted line). The spectra vary as they do for fused silica (Fig. 6H), but follow the pattern of broad emission spectra with few discernible lines. A reliable spectrum was not obtained for CaF_2 due to photo-bleaching. However, DKDP spectra were readily obtained. Note that after photo-brightening the DKDP spectrum shifted to the red significantly (green and dotted green lines in Fig. 6H).

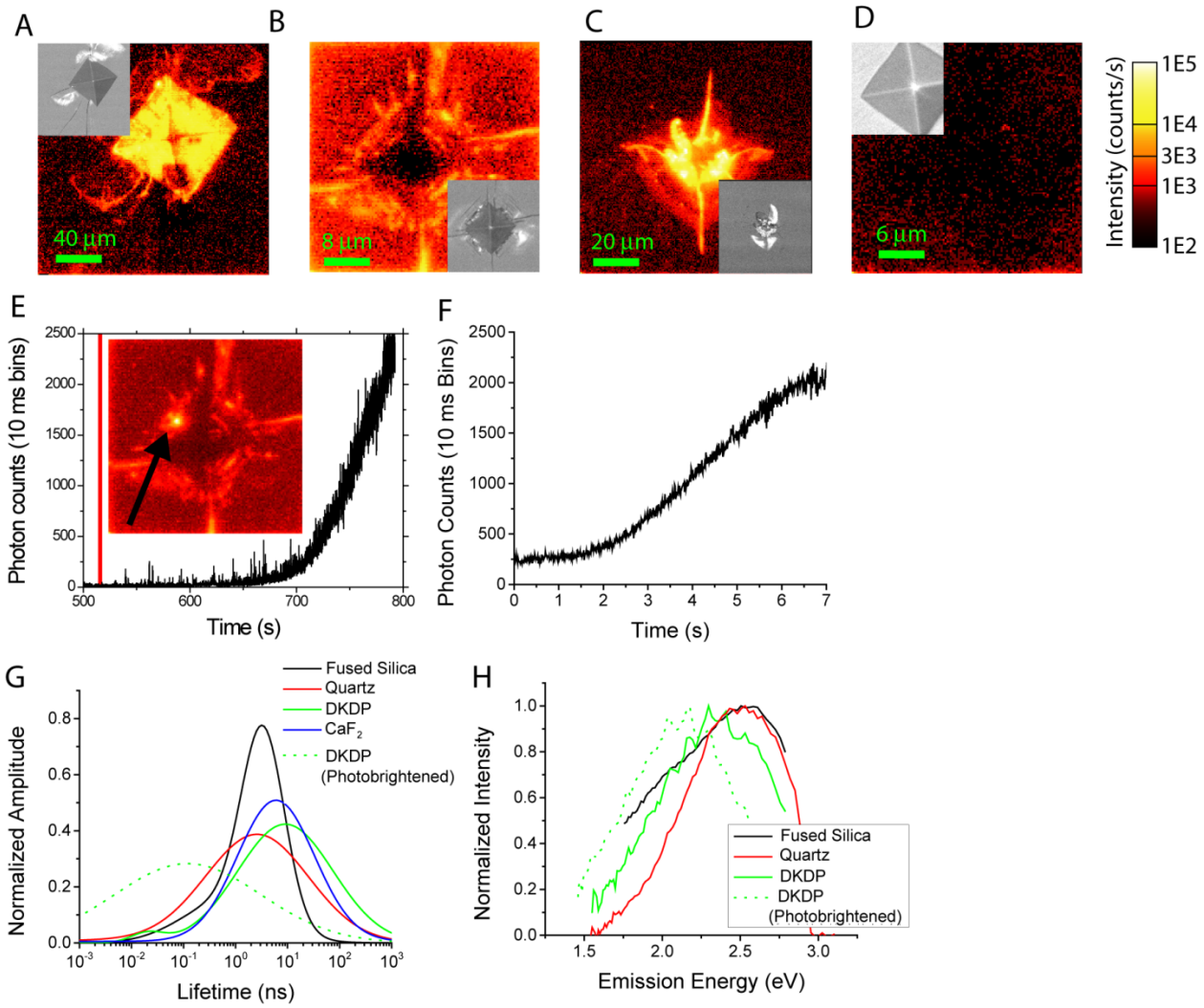

Figure 6: QC-PL characteristics are observed in other optical materials. **A**. 10 N indentation in CaF_2 exhibits quickly photo-bleaching QC-PL. Dark region near lower corner of indentation is due to photo-bleaching from a previous image. **B**. 0.5 N indentation in DKDP exhibiting QC-PL. **C**. 3 N indentation in quartz. **D**. A gentler 0.5 N indentation in CaF_2 does not exhibit QC-PL due to the lack of fractures. This shows that the PL observed in other cases is not due to contamination from the Vicker's indentation tip. **E**.

III. f. The PL is not simply due to contamination

Although contamination may contribute to the network of defects that can be excited, the origin of QC-PL is from defects in the structure of the materials themselves, rather than the presence of a foreign material. In addition to the indentation experiment in CaF_2 (Fig. 6D), we performed two experiments that verify that the PL is from the materials themselves, rather than from contamination from air or other sources over days. First, we formed the indentations and measured the QC-PL in less than one hour to show that the PL did not arise from storage overnight. We also performed a measurement of QC-PL on fused silica spheres crushed between two 5 cm fused silica vacuum window samples. The crushed silica spheres were only exposed to other silica surfaces. PL was not observed on the vacuum windows, and only a dim,

longer-lived PL was observed from the silica spheres. Measurements taken within 2 minutes of crushing the spheres showed extensive bright QC-PL.

IV. Discussion

QC-PL, observed in surface flaws of optical materials and in other materials with high defect density, has several unusual properties that distinguish it from PL from isolated point defects in solids such as the NBOHC and the oxygen-deficiency centers in silica, color centers in other solids and in chromophores, etc. Broad distributions of spectral and temporal characteristics that shift based on conditions and even to exposure to a probe laser beam are not amenable to standard spectroscopy, preventing reliable characterization and identification of specific, optically active defects. Additionally, similar QC-PL is found in a variety of materials. However, the similarity in the characteristics and dynamics from the QC-PL observed in different materials provides a clue to the origin of this type of PL. Based on these comparisons, and our previous suggestion that energy transfer processes give rise to the distribution of lifetimes observed[8], we suggest that QC-PL arises from a high density of defects. The densities are high enough that the energy levels of defects are distorted by the presence of other defects in addition to the temporal effects. Examples of the effects that may play a role in changing energy levels include Davydov splitting and excitons found in conjugated polymers and other high chromophore concentration effects [20–24].

The fact that we only observe QC-PL on surfaces supports the suggestion that QC-PL arises from high densities of defects, which are most likely to be found at surfaces. The localized nature of this PL on surfaces has required the use of high-sensitivity micro-spectroscopic techniques[1,2]. If there is PL from the bulk material, techniques with lower resolution or sensitivity would miss this PL. Most studies avoid such defective regions, which we believe is why this PL has not been identified previously as a characteristic PL which can be observed in many different circumstances.

The suggestion that the outlined QC-PL characteristics arise from effects of high defect densities is motivated by other factors. For example, QC-PL has been associated with regions with higher laser-induced damage susceptibility. Estimates of defect densities required to explain laser-induced damage of optical surfaces point to a very high defect density[1,2,8]. For example, laser damage occurs for a growing laser damage site at ~5 J/cm^2 for a 3 ns, 3.5 eV laser pulse. Laser damage sites must get to over 5,000K in order to cause the host material to absorb and produce laser-assisted absorption fronts[25]. The energy to heat the lattice must come from photons. Assuming no heat diffusion, the absorbance must be at least α_{min} = 1200 cm^{-1}. For 3.5 eV photons, raising the temperature from 300K to 5,000K requires the absorption without reemission of more than 10^{22} photon absorptions/cm^3. For comparison, the density of Si-O bonds is 5×10^{22} cm^{-3}. These estimates suggest that, in order to explain laser damage, defect densities must approach atomic densities in damage-prone surface flaws. Such high densities are consistent with our explanation of QC-PL as arising from high defect densities. Although we have made measurements only in optical materials, other nanoscale structures with high densities of defects may exhibit similar properties. It was noted earlier that the continuous shift in lifetime was observed previously in Si nanoparticle samples formed by implanting Si+ ions into silica[7]. Under this interpretation, QC-PL is a metric for defect concentration – hence a metric for optical energy deposition – and perhaps a probe for photo-chemical activity.

The photo-brightening process we discovered in surface flaws of optical materials is very unusual, and may help in understanding the origin of QC-PL. It is likely related to photo-induced chemical processes. Photo-brightening is not linear in laser intensity, suggesting a balance between two competing processes. Photo-brightening decreases the fluorescence lifetime, indicating that this process creates more defects over time. It is important to note that obtaining bright PL balances two factors: defect density and quantum efficiency. Increases in defect density do increase brightness in general, as long as quantum efficiency does not decrease dramatically. Quantum efficiency, the fraction of excitations that lead to fluorescence or PL rather than internal conversion or excitation transfer, often decreases at very high defect density, quenching PL. It may be the case that the brightest PL occurs at lower defect densitites. The fact that the photo-brightening coincides with a *decrease* in lifetime often associated with quenching indicates that there is a dramatic increase in the density of photo-active defects. In order to create a defect in photo-brightening, more than one photon is likely involved since the energy required to create a new defect in wide band gap materials is likely more than the 3 eV used for the probe laser, and since a strong non-linearity is observed in the rate of defect generation. Our intensities are not high enough to produce two- or three-photon absorption. However, multi-step processes may be involved in this process [26,27]. Also, given a very high density of defects, it is possible that two nearby excitation may undergo a process such as singlet-singlet annihilation[28], promoting one of the excitation to a much higher energy. Investigation of these processes will improve the understanding of the optical response processes of all materials surfaces at high defect density, not just in the case of laser-induced damage of optical materials.

The unusual properties of QC-PL have prevented their identification as a separate phenomenon. If our suggested hypothesis continues to be supported by further evidence, QC-PL will be relevant not only to surface flaws in optical materials, but on surfaces of any materials with high defect densities. The optical materials only provided the easiest way to identify QC-PL as a separate phenomenon since point defects in pure optical materials are well-characterized and relatively few. We believe further study of the properties and how they arise will be relevant to any surfaces with high densities of optically active defects.

Prepared by LLNL under Contract DE-AC52-07NA27344.

V. References

[1] T.A. Laurence, J.D. Bude, N. Shen, T. Feldman, P.E. Miller, W.A. Steele, and T. Suratwala, Appl. Phys. Lett. **94**, 151114 (2009).
[2] T.A. Laurence, J.D. Bude, N. Shen, P.E. Miller, W.A. Steele, G. Guss, J.J. Adams, L.L. Wong, M.D. Feit, and T.I. Suratwala, in (2009), pp. 750416–750416–11.
[3] P.E. Miller, J.D. Bude, T.I. Suratwala, N. Shen, T.A. Laurence, W.A. Steele, J. Menapace, M.D. Feit, and L.L. Wong, Opt. Lett. **35**, 2702 (2010).
[4] S.O. Kucheyev and S.G. Demos, Appl. Phys. Lett. **82**, 3230 (2003).
[5] J. Fournier, J. Neauport, P. Grua, E. Fargin, V. Jubera, D. Talaga, and S. Jouannigot, Appl. Phys. Lett. **100**, 114103 (2012).
[6] J. Fournier, J. Néauport, P. Grua, E. Fargin, V. Jubera, D. Talaga, and S. Jouannigot, Opt Express **18**, 21557 (2010).
[7] Y. Kanemitsu, N. Shimizu, T. Komoda, P.L. Hemment, and B.J. Sealy, Phys. Rev. B **54**, R14329 (1996).
[8] T.A. Laurence, J.D. Bude, and N. Shen, MRS Online Proc. Libr. **1365**, (2011).
[9] T. Förster, Naturwissenschaften **33**, 166 (1946).
[10] D.L. Dexter, J. Chem. Phys. **21**, 836 (1953).
[11] T. Förster, Z. Naturforschung Sect. - J. Phys. Sci. **4**, 321 (1949).

[12] A. Blumen, Nuovo Cimento Della Soc. Ital. Fis. B-Gen. Phys. Relativ. Astron. Math. Phys. Methods **63**, 50 (1981).
[13] J. Klafter and A. Blumen, J. Chem. Phys. **80**, 875 (1984).
[14] T.I. Suratwala, P.E. Miller, J.D. Bude, W.A. Steele, N. Shen, M.V. Monticelli, M.D. Feit, T.A. Laurence, M.A. Norton, C.W. Carr, and L.L. Wong, J. Am. Ceram. Soc. **94**, 416 (2011).
[15] T.A. Laurence and B.A. Chromy, Nat Meth **7**, 338 (2010).
[16] C. Zander, M. Sauer, K.H. Drexhage, D.-S. Ko, A. Schulz, J. Wolfrum, L. Brand, C. Eggeling, and C.A.M. Seidel, Appl. Phys. B **63**, 517 (1996).
[17] L. Skuja, J. Non-Cryst. Solids **179**, 51 (1994).
[18] L. Skuja, J. Non-Cryst. Solids **239**, 16 (1998).
[19] D. Gerion, F. Pinaud, S.C. Williams, W.J. Parak, D. Zanchet, S. Weiss, and A.P. Alivisatos, J. Phys. Chem. B **105**, 8861 (2001).
[20] T. Misra, Rev. Pure Appl. Chem. **15**, 39 (1965).
[21] P. Dawson, J. Phys. Chem. Solids **36**, 1401 (1975).
[22] F.C. Spano, Annu. Rev. Phys. Chem. **57**, 217 (2006).
[23] R.O. Al-Kaysi, T. Sang Ahn, A.M. M?ller, and C.J. Bardeen, Phys. Chem. Chem. Phys. **8**, 3453 (2006).
[24] E. Sagvolden, F. Furche, and A. Köhn, J. Chem. Theory Comput. **5**, 873 (2009).
[25] C. Carr, J. Bude, and P. DeMange, Phys. Rev. B **82**, (2010).
[26] S.G. Demos, Y. Takiguchi, and R.R. Alfano, Opt. Lett. **18**, 522 (1993).
[27] C. Carr, H. Radousky, and S. Demos, Phys. Rev. Lett. **91**, (2003).
[28] J. Hofkens, M. Cotlet, T. Vosch, P. Tinnefeld, K.D. Weston, C. Ego, A. Grimsdale, K. Müllen, D. Beljonne, and J.L. Brédas, Proc. Natl. Acad. Sci. **100**, 13146 (2003).